VIBRATION AND SHAPE CONTROL OF COMPOSITE PIEZOELECTRIC PLATES

Fernanda Colnago Gomes da Silva, fernandacolnago@gmail.com
Universidade Federal de Santa Catarina, Departamento de Engenharia Mecânica - Campus Universitário Trindade, 88040 - 900, Florianópolis - SC

Nicolas Palluat, nicolas@ita.br
Instituto Tecnológico de Aeronáutica, Divisão de Engenharia Eletrônica, 12228 - 900 São José dos Campos - SP, Brasil

Marcelo Krajnc Alves, krajnc@emc.ufsc.br
Universidade Federal de Santa Catarina, Departamento de Engenharia Mecânica - Campus Universitário Trindade, 88040 - 900, Florianópolis - SC

Abstract. *This work proposes a theoretical approach and a numerical scheme for the vibration control of composite piezoelectric plates. The first order Mindlin theory for laminated plate is employed together with the coupling electromechanical effect due to the use of laminae of piezoelectric materials for vibration control. The discretization of the problem is done by the Galerkin finite element method. The piezoelectric laminae work as actuators and sensors. The proposed approach considers the piezoelectric material presents linear behaviour and derives consistently the coupled electromechanical equations and associated boundary conditions. The discrete dynamical response of the structure is computed by the Newmark method. In order to perform the vibration control of the plate structures a simple PID (proportional-integral-derivative control system) control system is applied. The validation of the model and numerical scheme is done by comparing the derived solution with analytical and numerical solutions, obtained by using the ANSYS® code.*

Keywords: *Vibration Control, Shape Control, Piezoelectric Composite plate, Proportional-integral-derivative control system.*

1. INTRODUCTION

In these last years, the technology evolve to reduce the number of components in systems (to reduce size, weight, . . .). In this context, the study and development of new materials with physical characteristics capable to realize multiple tasks increase. Smart materials, like shape memory alloy and piezoelectric materials, improve systems in terms of efficiency, size, weight, noise and reduce the number of supplementary parts, such as sensors and actuators, used in control systems. Many areas, such as aeronautical and automobile industries, employ these materials in devices to suppress structural vibrations and in sensoring/positioning systems.

Several strategies were used in order to describe mathematically piezoelectric material behaviour and to develop numerical models. Adriaens et al. (2000) and da Silva (2005) used transfer function models to describe system dynamics. An another approach to simulate piezoelectric materials is the Finite Element Method (FEM), used in the greater part of studies (Lam et al., 1997; Reddy, 1999). Different kinds of structures have been modelled, using piezoelectric material only or assembled with isotropic or orthotropic materials.

This work deals with the vibration problem in laminate composite plates. In order to reduce vibrations, piezoelectric sensors and actuators were bonded in plate surfaces considering their coupled electromechanical effect. The first order plate theory was employed to create a mathematical model of the resulting structure. A Finite Element Model is proposed and system dynamics is obtained using Newmark method. The validation is made by comparison of results with analytical and numerical solutions, obtained by using the software ANSYS®. Active feedback control is performed using a PID controller.

2. PIEZOELECTRIC AND COMPOSITE MATERIALS

Piezoelectric and composite materials are orthotropic, so it is necessary to define $\{\vec{e}_1, \vec{e}_2, \vec{e}_3\}$ as orthotropy axes and $\{\vec{e}_1, \vec{e}_2\}$ as lamina axes. This model considers a perfect bonding between layers, i.e., continuous displacements and strains through plate thickness. The constitutive equations for piezoelectric materials are presented in Eq. 1. For composite materials equations, the electromechanical coupling of the constitutive equations must be suppressed.

$$\begin{aligned} \sigma &= c^E\,\varepsilon - e^T\,E \\ D &= e\,\varepsilon + \epsilon_D^{\varepsilon}\,E \end{aligned} \tag{1}$$

where σ, ε, D and E are mechanical stress, mechanical strain, electric displacement and electric field, respectively. Matrix c provides the elastic constants, e denotes the piezoelectric stress coefficients and ϵ_D, the dielectric matrix. The

superscript ε means that values are measured at constant mechanical strain and superscript E means that values are measured at constant electric field. Due to orthotropy, constitutive equations for a piezoelectric material in lamina reference system can be defined as shown in Eq. 2.

$$\begin{Bmatrix}\sigma_{11}\\ \sigma_{22}\\ \sigma_{33}\\ \sigma_{23}\\ \sigma_{13}\\ \sigma_{12}\end{Bmatrix} = \begin{bmatrix} c_{11}^E & c_{12}^E & c_{13}^E & 0 & 0 & 0\\ c_{12}^E & c_{22}^E & c_{23}^E & 0 & 0 & 0\\ c_{13}^E & c_{23}^E & c_{33}^E & 0 & 0 & 0\\ 0 & 0 & 0 & c_{44}^E & 0 & 0\\ 0 & 0 & 0 & 0 & c_{55}^E & 0\\ 0 & 0 & 0 & 0 & 0 & c_{66}^E \end{bmatrix} \begin{Bmatrix}\varepsilon_{11}\\ \varepsilon_{22}\\ \varepsilon_{33}\\ \gamma_{23}\\ \gamma_{13}\\ \gamma_{12}\end{Bmatrix} - \begin{bmatrix} 0 & 0 & e_{31}\\ 0 & 0 & e_{32}\\ 0 & 0 & e_{33}\\ 0 & e_{24} & 0\\ e_{15} & 0 & 0\\ 0 & 0 & 0 \end{bmatrix} \begin{Bmatrix}E_1\\ E_2\\ E_3\end{Bmatrix}$$

$$\begin{Bmatrix}D_1\\ D_2\\ D_3\end{Bmatrix} = \begin{bmatrix} 0 & 0 & 0 & 0 & e_{15} & 0\\ 0 & 0 & 0 & e_{24} & 0 & 0\\ e_{31} & e_{32} & e_{33} & 0 & 0 & 0 \end{bmatrix} \begin{Bmatrix}\varepsilon_{11}\\ \varepsilon_{22}\\ \varepsilon_{33}\\ \gamma_{23}\\ \gamma_{13}\\ \gamma_{12}\end{Bmatrix} + \begin{bmatrix} \epsilon_{D_{11}}^{\varepsilon} & 0 & 0\\ 0 & \epsilon_{D_{22}}^{\varepsilon} & 0\\ 0 & 0 & \epsilon_{D_{33}}^{\varepsilon} \end{bmatrix} \begin{Bmatrix}E_1\\ E_2\\ E_3\end{Bmatrix} \tag{2}$$

Once this study applies Mindlin theory, it is necessary to use plane-stress condition, where $\sigma_{33} = \sigma_{23} = \sigma_{13} = 0$. However, shear components are still considered. The correspondent matrix line to σ_{33} defines the relation described in Eq. 3.

$$\varepsilon_{33} = -\frac{1}{c_{33}^E}\left(c_{13}^E\varepsilon_{11} + c_{23}^E\varepsilon_{22}\right) + \frac{e_{33}}{c_{33}^E}E_3 \tag{3}$$

Substituting Eq. 3 in constitutive equation Eq. 2 results in Eq. 4.

$$\begin{bmatrix} C_{11} & C_{12}\\ C_{12} & C_{22}\end{bmatrix} = \begin{bmatrix} c_{11}^E & c_{12}^E\\ c_{12}^E & c_{22}^E\end{bmatrix} - \frac{1}{c_{33}^E}\left[\begin{Bmatrix} c_{13}^E\\ c_{23}^E\end{Bmatrix} \otimes \begin{Bmatrix} c_{13}^E\\ c_{23}^E\end{Bmatrix}\right] \tag{4}$$

Assuming $C_{33} = c_{66}^E$, a more complete constitutive equation can be found (Eq. 5).

$$\begin{Bmatrix}\sigma_{11}\\ \sigma_{22}\\ \sigma_{12}\\ \sigma_{23}\\ \sigma_{13}\end{Bmatrix} = \begin{bmatrix} C_{11} & C_{12} & 0 & 0 & 0\\ C_{12} & C_{22} & 0 & 0 & 0\\ 0 & 0 & C_{33} & 0 & 0\\ 0 & 0 & 0 & c_{44}^E & 0\\ 0 & 0 & 0 & 0 & c_{55}^E \end{bmatrix} \begin{Bmatrix}\varepsilon_{11}\\ \varepsilon_{22}\\ \gamma_{12}\\ \gamma_{23}\\ \gamma_{13}\end{Bmatrix} - \begin{bmatrix} 0 & 0 & e_{31M}\\ 0 & 0 & e_{32M}\\ 0 & 0 & 0\\ 0 & e_{24} & 0\\ e_{15} & 0 & 0 \end{bmatrix} \begin{Bmatrix}E_1\\ E_2\\ E_3\end{Bmatrix}$$

$$\begin{Bmatrix}D_1\\ D_2\\ D_3\end{Bmatrix} = \begin{bmatrix} 0 & 0 & 0 & 0 & e_{15}\\ 0 & 0 & 0 & e_{24} & 0\\ e_{31M} & e_{32M} & 0 & 0 & 0 \end{bmatrix} \begin{Bmatrix}\varepsilon_{11}\\ \varepsilon_{22}\\ \gamma_{12}\\ \gamma_{23}\\ \gamma_{13}\end{Bmatrix} + \begin{bmatrix} \epsilon_{D_{11}}^{\varepsilon} & 0 & 0\\ 0 & \epsilon_{D_{22}}^{\varepsilon} & 0\\ 0 & 0 & \epsilon_{D_{33M}}^{\varepsilon} \end{bmatrix} \begin{Bmatrix}E_1\\ E_2\\ E_3\end{Bmatrix} \tag{5}$$

with $e_{31M} = e_{31} - \frac{c_{13}^E}{c_{33}^E}e_{33}$, $e_{32M} = e_{32} - \frac{c_{23}^E}{c_{33}^E}e_{33}$ and $\epsilon_{D_{33M}}^{\varepsilon} = \epsilon_{D_{33}}^{\varepsilon} + \frac{e_{33}^2}{c_{33}^E}$.

3. ASSUMPTIONS ABOUT MECHANICAL AND ELECTROMECHANICAL MODELS

(i) Mindlin first order theory considers the following displacement field in global coordinate system $\{x, y, z\}$:

$$U(x,y) = u(x,y) + z\theta_y(x,y), \quad V(x,y) = v(x,y) - z\theta_x(x,y), \quad W(x,y) = w(x,y) \tag{6}$$

where θ_x and θ_y represent the rotation around the x- and y-dimensions respectively, and u, v and w the displacement along x-, y- and z-directions, respectively.

(ii) Normal stress to laminate plane $\sigma_{zz} \simeq 0$ and the plane-stress condition is applied.

(iii) Electric field is uniform through piezoelectric layer thickness and is normal to lamina plane, aligned to direction $\vec{e}_z$. This vector is represented in Eq. 7.

$$\vec{E} = \begin{Bmatrix} 0 & 0 & E_z\end{Bmatrix}^T \quad \text{where } E_x = E_y = 0 \tag{7}$$

The components of strain tensor can be found using the relations in Eq. 8.

$$\begin{aligned}
\varepsilon_{xx} &= \frac{\partial U}{\partial x} = \frac{\partial u}{\partial x} + z\frac{\partial \theta_y}{\partial x} = \varepsilon^o_{xx} + z\,\kappa_{xx}, \quad & \gamma_{xz} &= \frac{\partial U}{\partial z} + \frac{\partial W}{\partial x} = \theta_y + \frac{\partial w}{\partial x} \\
\varepsilon_{yy} &= \frac{\partial V}{\partial y} = \frac{\partial v}{\partial y} - z\frac{\partial \theta_x}{\partial y} = \varepsilon^o_{yy} + z\,\kappa_{yy}, \quad & \gamma_{yz} &= \frac{\partial V}{\partial z} + \frac{\partial W}{\partial y} = -\theta_x + \frac{\partial w}{\partial y} \\
\varepsilon_{zz} &= 0, & \gamma_{xy} &= \left[\frac{\partial U}{\partial y} + \frac{\partial V}{\partial x}\right] = \left[\frac{\partial u}{\partial y} + \frac{\partial v}{\partial x}\right] + z\left[\frac{\partial \theta_y}{\partial y} - \frac{\partial \theta_x}{\partial x}\right] = \gamma^o_{xy} + z\,\kappa_{xy}
\end{aligned} \tag{8}$$

Laminate structure is presented in Fig. 1(a). Composite fibres are related to x axis and piezoelectric polarization is along z axis. Figure 1(b) shows a schematic representation of stacking sequence. Layers 1 and N are piezoelectric laminae bonded on composite laminate surfaces.

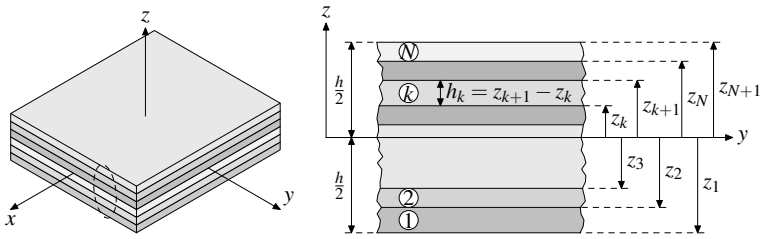

(a) Laminate structure (b) Stacking overview

Figure 1. Identification criteria of stacking sequence

Considering equilibrium equation defined in its weak form,

$$\int_\Omega \sigma.\varepsilon\left(\delta\vec{u}\right)\, d\Omega + \int_\Omega \rho\, \overrightarrow{\ddot{u}}.\delta\vec{u}\, d\Omega = \int_\Omega \rho\, \vec{g}.\delta\vec{u}\, d\Omega + \int_{\partial_t\Omega} \overrightarrow{t}\,.\delta\vec{u}\, d\partial_t\Omega \tag{9}$$

and applying relations established in Eq. 8, leads to Eq. 10.

$$\begin{aligned}
\int_\Omega \sigma(u).\varepsilon\left(\delta\vec{u}\right) d\Omega = \int_A \int_{\frac{-h}{2}}^{\frac{h}{2}} \Big\{ & \sigma_{xx}\left[\delta\varepsilon^o_{xx} + z\delta\kappa_{xx}\right] + \sigma_{yy}\left[\delta\varepsilon^o_{yy} + z\delta\kappa_{yy}\right] \\
& + \sigma_{xy}\left[\delta\gamma^o_{xy} + z\delta\kappa_{xy}\right] + a\left(\sigma_{yz}\delta\gamma_{yz} + \sigma_{xz}\delta\gamma_{xz}\right)\Big\}\, dzdA
\end{aligned} \tag{10}$$

where h is lamina thickness and a is a energy correction factor for transversal shear strain ($a = \frac{5}{6}$). Generalized membrane, bending and normal forces are formulated as,

$$\begin{aligned}
N_{xx} &= \int_{\frac{-h}{2}}^{\frac{h}{2}} \sigma_{xx} dz, \quad & N_{yy} &= \int_{\frac{-h}{2}}^{\frac{h}{2}} \sigma_{yy} dz, \quad & N_{xy} &= \int_{\frac{-h}{2}}^{\frac{h}{2}} \sigma_{xy} dz, \quad & Q_{xz} &= a\int_{\frac{-h}{2}}^{\frac{h}{2}} \sigma_{xz} dz \\
M_{xx} &= \int_{\frac{-h}{2}}^{\frac{h}{2}} z\sigma_{xx} dz, \quad & M_{yy} &= \int_{\frac{-h}{2}}^{\frac{h}{2}} z\sigma_{yy} dz, \quad & M_{xy} &= \int_{\frac{-h}{2}}^{\frac{h}{2}} z\sigma_{xy} dz, \quad & Q_{yz} &= a\int_{\frac{-h}{2}}^{\frac{h}{2}} \sigma_{yz} dz
\end{aligned} \tag{11}$$

Defining generalized loading $\vec{C_g}$ and generalized strain $\vec{D_g}$ vectors,

$$\vec{C_g} = \left\{N_{xx}, N_{yy}, N_{xy}, M_{xx}, M_{yy}, M_{xy}, Q_{yz}, Q_{xz}\right\}^T \qquad \text{and} \qquad \vec{D_g} = \left\{\varepsilon^o_{xx}, \varepsilon^o_{yy}, \gamma^o_{xy}, \kappa_{xx}, \kappa_{yy}, \kappa_{xy}, \gamma_{yz}, \gamma_{xz}\right\} \tag{12}$$

The equilibrium equation, already integrated in lamina thickness, is reported in Eq. 13.

$$\begin{aligned}
&\int_A \vec{C_g}.\delta\vec{D_g}\, dA + \int_A \sum_{k=1}^{n} \left\{\rho^k h_{k,1}\right\} \overrightarrow{\ddot{u}}_0.\delta\vec{u}_0 dA + \int_A \sum_{k=1}^{n} \left\{\rho^k h_{k,3}\right\} \overrightarrow{\ddot{\theta}}\,.\delta\vec{\theta} dA - \\
&\int_A \sum_{k=1}^{n} \left\{\rho^k h_{k,2}\right\} \left(\overrightarrow{\ddot{u}}_0.\delta\vec{\theta} + \overrightarrow{\ddot{\theta}}\,.\delta\vec{u}_0\right) dA = \int_{\partial A_t} \left\{\overrightarrow{\overline{N}}.\delta\vec{u}_0 - \overrightarrow{\overline{M}}.\delta\vec{\theta}\right\} dA + \\
&\qquad \int_A \sum_{k=1}^{n} \left\{\rho^k h_{k,1}\right\} \vec{g}.\vec{u}_0\, dA - \int_A \sum_{k=1}^{n} \left\{\rho^k h_{k,2}\right\}\, \vec{g}.\delta\vec{\theta}\, dA
\end{aligned} \tag{13}$$

where the constants $h_{k,1}$, $h_{k,2}$ e $h_{k,3}$ are declared as,

$$h_{k,1} = z_{k+1} - z_k; \qquad h_{k,2} = \frac{\left(z_{k+1}^2 - z_k^2\right)}{2}; \qquad h_{k,3} = \frac{\left(z_{k+1}^3 - z_k^3\right)}{3} \tag{14}$$

and

$$\overrightarrow{\overrightarrow{N}} = \int_{\frac{-h}{2}}^{\frac{h}{2}} \vec{\vec{t}} dz \qquad \text{and} \qquad \overrightarrow{\overrightarrow{M}} = \int_{\frac{-h}{2}}^{\frac{h}{2}} z\, \vec{\vec{t}} dz \tag{15}$$

The constitutive equation, grouping terms of shear and in-plane forces (membrane and bending), can be re-written in compact form according to Eq. 16.

$$\begin{bmatrix} \vec{\sigma_p}^{(k)} \\ \vec{\sigma_s}^{(k)} \end{bmatrix} = \begin{bmatrix} \left[\overline{C}_p^{(k)}\right] & \left[0\right] \\ \left[0\right] & \left[\overline{C}_s^{(k)}\right] \end{bmatrix} \begin{bmatrix} \vec{\varepsilon_p}^{(k)} \\ \vec{\gamma_s}^{(k)} \end{bmatrix} + \begin{bmatrix} \left[\overline{e}_p^{(k)}\right] \\ \left[\overline{e}_s^{(k)}\right] \end{bmatrix} \vec{E}^{(k)} \tag{16}$$

Relating Eq. 16 to Eq. 8 and defining the vectors,

$$\vec{\varepsilon_p^o}^{(k)} = \left\{ {\varepsilon_{xx}^o}^{(k)} \quad {\varepsilon_{yy}^o}^{(k)} \quad {\gamma_{xy}^o}^{(k)} \right\}^T \quad \text{and} \quad \left(\vec{\kappa}_p\right)^{(k)} = \left\{ {\kappa_{xx}}^{(k)} \quad {\kappa_{yy}}^{(k)} \quad {\kappa_{xy}}^{(k)} \right\}^T \tag{17}$$

a relation between generalized forces and strain field can be established,

$$\begin{aligned} \vec{N} &= \sum_{k=1}^{n} \left[\overline{C}_p^{(k)}\right] h_{k,1} \vec{\varepsilon_p^o}^{(k)} + \sum_{k=1}^{n} \left[\overline{C}_p^{(k)}\right] h_{k,2} \vec{\kappa}_p^{(k)} + \sum_{k=1}^{n} \left[\overline{e}_p^{(k)}\right] h_{k,1} \vec{E}^{(k)} \\ \vec{M} &= \sum_{k=1}^{n} \left[\overline{C}_p^{(k)}\right] h_{k,2} \vec{\varepsilon_p^o}^{(k)} + \sum_{k=1}^{n} \left[\overline{C}_p^{(k)}\right] h_{k,3} \vec{\kappa_p}^{(k)} + \sum_{k=1}^{n} \left[\overline{e}_p^{(k)}\right] h_{k,2} \vec{E}^{(k)} \\ \vec{Q} &= a \sum_{k=1}^{n} \left[\overline{C}_s^{(k)}\right] h_{k,1} \vec{\gamma_s}^{(k)} + \sum_{k=1}^{n} a \left[\overline{e}_s^{(k)}\right] h_{k,1} \vec{E}^{(k)} \end{aligned} \tag{18}$$

So, the generalized load $\vec{C_g}$ is described in compact form, as,

$$\vec{C_g} = \begin{Bmatrix} \vec{N} \\ \vec{M} \\ \vec{Q} \end{Bmatrix} = \begin{bmatrix} \mathbb{D}_P & 0 \\ 0 & \mathbb{D}_S \end{bmatrix} \vec{D_g} + \sum_{k=1}^{n} \left[\mathbb{E}_{PS}\right] \vec{E} \tag{19}$$

where $\mathbb{D}_P$, $\mathbb{D}_S$ and $\mathbb{E}_{PS}$ are matrices related terms to in-plane stresses, transversal shear stresses and electric field, respectively.

4. CONSIDERATIONS ABOUT THE ELECTRIC FIELD AND ITS POTENTIAL

In order to model electric potential distribution through piezoelectric lamina thickness, the following assumptions are considered, according to Bhattacharya (2006):

(i) The potential distribution through lamina thickness is linear;

(ii) The piezoelectric surfaces in contact with composite layer are grounded, so electric potential between different material surfaces is zero;

(iii) Bondings between piezoelectric layer, electrode and composite material are perfect.

Extra assumption are assumed:

(iv) No piezoelectric layer between composite laminae;

(v) Composite material is considered non dielectric;

(vi) Piezoelectric sensors and actuators are always symmetrically bonded on composite laminate surface;

(vii) Electric potential in each layer is homogeneous along its plane.

Due to these considerations, the electric potential of a layer can be described as,

$$\varphi^{(k)}(x,y,z) = \overline{\varphi}^{(k)}(x,y)\,\frac{(z-z_k)}{(z_{k+1}-z_k)} \text{ and, in each lamina, } \left.\overline{\varphi}^{(k)}(x,y)\right|_{lam} = cte \tag{20}$$

So, the electric field and its potential are related as,

$$\left.\vec{E}^{(k)}(x,y,z)\right|_{lam} = -\nabla\varphi^{(k)}(x,y,z) = -\frac{\left.\overline{\varphi}^{(k)}(x,y)\right|_{lam}}{h_{k,1}}\vec{e}_z = -\frac{\left.\overline{\varphi}^{(k)}\right|_{lam}}{h_{k,1}}\vec{e}_z = cte \tag{21}$$

Once the relations between electrical entities are defined, the second equation derived from the electromechanical weak form is formulated in Eq. 22

$$\int_\Omega \vec{D}.\nabla\delta\varphi\; d\Omega = \int_{\partial_\psi\Omega} \overline{\psi}\delta\varphi\; d\partial_\psi\Omega \tag{22}$$

where $\vec{D}$ is known from the second equation of constitutive equation (Eq. 5). Using Eq. 21 and Eq. 5 in Eq. 22, the electrical equilibrium equation integrated in laminate thickness is determined (Eq. 23).

$$\int_A \left\{\sum_{k=1}^{n}\left[\overline{\epsilon_D^{\varepsilon}}^{(k)}\right] h_{k,1}\vec{E}^{(k)}.\delta\vec{E}^{(k)}\right\} dA + \int_A \sum_{k=1}^{n}\left[\mathbb{E}_{PS}\right]^T \vec{D}_g.\delta\vec{E}^{(k)}dA = -\int_{\partial A_\psi}\overline{\psi}z_k h_{k,1}\vec{e}_z.\delta\vec{E}^{(k)}dA \tag{23}$$

Once the electromechanical formulation problem is completely represented, finite element discretization is applied.

5. FINITE ELEMENT DISCRETIZATION

This work was developed using isoparametric element $Quad9$, with $(u, v, w, \theta_y, -\theta_x)$ as degrees of freedom per node. For piezoelectric material, additionals degrees of freedom associated to electric potential are used ($\bar{\varphi}$), where the superscripts 1 and N refers to actuator and sensor layers, according to Figure 1(b). So, for a structure with upper and lower piezoelectric layers, the vector of degrees of freedom per elements can be expressed as,

$$\vec{q}_e^{\,T} = \left\{u_1, v_1, w_1, \theta_{y_1}, -\theta_{x_1}, \ldots, u_9, v_9, w_9, \theta_{y_9}, -\theta_{x_9}, \bar{\varphi}^1, \bar{\varphi}^N\right\} \tag{24}$$

In order to avoid shear locking, selective reduced integration method is used. Then, 9 integration points are used for membrane and bending terms and 4 points for transversal shear terms. Relating equilibrium equations obtained by the discrete weak form formulation, displacements and virtual displacements are declared according to Eq. 25.

$$t^k(\vec{x}) = \sum_{i=1}^{9}\mathbb{N}_i(\xi,\eta)t_i, \qquad \delta t^k(\vec{x}) = \sum_{i=1}^{9}\mathbb{N}_i(\xi,\eta)\delta t_i \tag{25}$$

where t represents each degree of freedom, δt their virtual displacement and $\{\xi, \eta\}$ is coordinate system of element domain. Form functions $\mathbb{N}_i$ can be found in (Bathe and Wilson, 1976). So, discrete displacement vector $\vec{u}_0^k$ and its virtual displacement can be described in matrix form as,

$$\vec{u}_0^k(\vec{x}) = \left[\mathbb{N}_1^u(\xi,\eta)\middle|\mathbb{N}_2^u(\xi,\eta)\middle|\cdots\middle|\mathbb{N}_9^u(\xi,\eta)\middle|\left[0\right]\right]\left\{\vec{q}_e\right\} \tag{26}$$

where,

$$\left[\mathbb{N}^u(\xi,\eta)\right] = \begin{bmatrix}\mathbb{N}_i(\xi,\eta) & 0 & 0 & 0 & 0\\ 0 & \mathbb{N}_i(\xi,\eta) & 0 & 0 & 0\\ 0 & 0 & \mathbb{N}_i(\xi,\eta) & 0 & 0\end{bmatrix} \quad \text{and} \quad \left[0\right] = \begin{bmatrix}0 & 0\\ 0 & 0\\ 0 & 0\end{bmatrix} \tag{27}$$

and rotations can be defined as,

$$\vec{\theta^k} = \left[\mathbb{N}_1^\theta(\xi,\eta)\middle|\mathbb{N}_2^\theta(\xi,\eta)\middle|\cdots\middle|\mathbb{N}_9^\theta(\xi,\eta)\middle|\left[0\right]\right]\left\{\vec{q}_e\right\} \quad \text{where} \quad \left[\mathbb{N}^\theta(\xi,\eta)\right] = \begin{bmatrix}0 & 0 & 0 & -\mathbb{N}_i(\xi,\eta) & 0\\ 0 & 0 & 0 & 0 & \mathbb{N}_i(\xi,\eta)\end{bmatrix} \tag{28}$$

Once discrete displacements and rotations are known, the generalized strain vector is expressed as,

$$\vec{D_g} = \left[\mathbb{B}_1(\vec{x}(\xi,\eta))\middle|\mathbb{B}_2(\vec{x}(\xi,\eta))\middle|\cdots\middle|\mathbb{B}_9(\vec{x}(\xi,\eta))\middle|\left[0\right]\right]\left\{\vec{q}_e\right\} \tag{29}$$

where $\mathbb{B}_i$ is the matrix presented in Eq. 30.

$$\mathbb{B}_i\left(\vec{x}\left(\xi,\eta\right)\right)=\begin{bmatrix}\frac{\partial}{\partial x}\mathbb{N}_i(\xi,\eta) & 0 & 0 & 0 & 0\\ 0 & \frac{\partial}{\partial y}\mathbb{N}_i(\xi,\eta) & 0 & 0 & 0\\ \frac{\partial}{\partial y}\mathbb{N}_i(\xi,\eta) & \frac{\partial}{\partial x}\mathbb{N}_i(\xi,\eta) & 0 & 0 & 0\\ 0 & 0 & 0 & \frac{\partial}{\partial x}\mathbb{N}_i(\xi,\eta) & 0\\ 0 & 0 & 0 & 0 & -\frac{\partial}{\partial y}\mathbb{N}_i(\xi,\eta)\\ 0 & 0 & 0 & \frac{\partial}{\partial y}\mathbb{N}_i(\xi,\eta) & -\frac{\partial}{\partial x}\mathbb{N}_i(\xi,\eta)\\ 0 & 0 & \frac{\partial}{\partial y}\mathbb{N}_i(\xi,\eta) & 0 & -\mathbb{N}_i(\xi,\eta)\\ 0 & 0 & \frac{\partial}{\partial x}\mathbb{N}_i(\xi,\eta) & \mathbb{N}_i(\xi,\eta) & 0\end{bmatrix} \tag{30}$$

The determination of discrete electric field is obtained as follows,

$$\begin{Bmatrix}E_3^1\\ E_3^N\end{Bmatrix}=\left[[0_\varphi]\middle|[0_\varphi]\middle|\cdots\middle|[0_\varphi]\middle|[\mathbb{B}^\varphi]\right]\left\{\vec{q}_e\right\} \tag{31}$$

where $[0_\varphi]$ and $[\mathbb{B}^\varphi\left(\xi,\eta\right)]$ components are,

$$[0_\varphi]=\begin{bmatrix}0 & 0 & 0 & 0 & 0\\ 0 & 0 & 0 & 0 & 0\end{bmatrix} \qquad \text{and} \qquad [\mathbb{B}^\varphi]=\begin{bmatrix}\frac{1}{h_{1,1}} & 0\\ 0 & \frac{1}{h_{N,1}}\end{bmatrix} \tag{32}$$

The discrete relations are introduced in equilibrium equations defined in Eq. 13 and Eq. 23. Integrations in element domain are solved by numerical integration using Gauss-Legendre quadrature (Eq. 33).

$$\int_{-1}^{1}\int_{-1}^{1} f(\xi,\eta)d\xi d\eta \simeq \sum_{i=1}^{npt}\sum_{j=1}^{npt} f(\xi_i,\eta_j)W_iW_j \tag{33}$$

where W_i and W_j are defined by the number of integration points npt. The results for each term of the first and second equilibrium equation are exposed in Tables 1 and 2, respectively. The matrix $J(\xi_i,\eta_j)$ is the Jacobian, τ_i is related to prescribed forces in contour and $\mathbb{P}$, $\mathbb{Z}$ and $\overline{\Psi}$ are defined in Eq. 34.

Table 1. Numerical integration for terms of first equilibrium equation using Gauss-Legendre quadrature

Matrices	Numerical integration
$\left[\mathbb{K}_e^P\right]$	$\sum_{i=1}^{npt}\sum_{j=1}^{npt}\left[\mathbb{B}^p\left(\vec{x}(\xi_i,\eta_j)\right)\right]^T\left[\mathbb{D}_P\right]\left[\mathbb{B}^p\left(\vec{x}(\xi_i,\eta_j)\right)\right]J(\xi_i,\eta_j)W_iW_j$
$\left[\mathbb{K}_e^S\right]$	$\sum_{i=1}^{npt}\sum_{j=1}^{npt}\left[\mathbb{B}^s\left(\vec{x}(\xi_i,\eta_j)\right)\right]^T\left[\mathbb{D}_S\right]\left[\mathbb{B}^s\left(\vec{x}(\xi_i,\eta_j)\right)\right]J(\xi_i,\eta_j)W_iW_j$
$\left[\mathbb{H}_e^{qu}\right]$	$\sum_{i=1}^{npt}\sum_{j=1}^{npt}\left[\mathbb{B}\left(\vec{x}(\xi_i,\eta_j)\right)\right]^T\left[\mathbb{P}\right]\left[\mathbb{B}^\varphi\left(\vec{x}(\xi_i,\eta_j)\right)\right]J(\xi_i,\eta_j)W_iW_j$
$\left[\mathbb{M}_e^u\right]$	$\sum_{i=1}^{npt}\sum_{j=1}^{npt}\left(\sum_{k=1}^{n}\left\{\rho^k h_{k,1}\right\}\left[\mathbb{N}^u\left(\xi_i,\eta_j\right)\right]^T\left[\mathbb{N}^u\left(\xi_i,\eta_j\right)\right]J(\xi_i,\eta_j)W_iW_j\right)$
$\left[\mathbb{M}_e^\theta\right]$	$\sum_{i=1}^{npt}\sum_{j=1}^{npt}\left(\sum_{k=1}^{n}\left\{\rho^k h_{k,3}\right\}\left[\mathbb{N}^\theta\left(\xi_i,\eta_j\right)\right]^T\left[\mathbb{N}^\theta\left(\xi_i,\eta_j\right)\right]J\left(\xi_i,\eta_j\right)W_iW_j\right)$
$\left[\mathbb{M}_e^{u\theta}\right]$	$\sum_{i=1}^{npt}\sum_{j=1}^{npt}\left(\sum_{k=1}^{n}\left\{\rho^k h_{k,2}\right\}\left\{\left[\mathbb{N}^\theta\left(\xi_i,\eta_j\right)\right]^T\left[\mathbb{N}^u\left(\xi_i,\eta_j\right)\right]+\left[\mathbb{N}^u\left(\xi_i,\eta_j\right)\right]^T\left[\mathbb{N}^\theta\left(\xi_i,\eta_j\right)\right]\right\}J(\xi_i,\eta_j)\right)W_iW_j$
$\vec{F}_e^{gu}$	$\sum_{i=1}^{npt}\sum_{j=1}^{npt}\left(\sum_{k=1}^{n}\left\{\rho^k h_{k,1}\right\}\left[\mathbb{N}^u\left(\xi_i,\eta_j\right)\right]^T\vec{g}\,J(\xi_i,\eta_j)W_iW_j\right)$
$\vec{F}_e^{g\theta}$	$\sum_{i=1}^{npt}\sum_{j=1}^{npt}\left(\sum_{k=1}^{n}\left\{\rho^k h_{k,2}\right\}\left[\mathbb{N}^\theta\left(\xi_i,\eta_j\right)\right]^T\vec{g}\,J(\xi_i,\eta_j)W_iW_j\right)$
$\vec{F}_e^N$	$\sum_{i=1}^{npt}\left[\mathbb{N}^u\left(\tau_i\right)\right]^T\overrightarrow{N}\,J\left(\tau_i\right)W_i$
$\vec{F}_e^M$	$\sum_{i=1}^{npt}\left[\mathbb{N}^\theta\left(\tau_i\right)\right]^T\overrightarrow{M}\,J\left(\tau_i\right)W_i$

$$[\mathbb{P}]=\begin{bmatrix}\overrightarrow{\mathbb{E}_{PS}^{(1)}}(:,3)\\ \overrightarrow{\mathbb{E}_{PS}^{(N)}}(:,3)\end{bmatrix}^T \quad [\mathbb{Z}]=\begin{bmatrix}h_{1,1}\overline{\epsilon_{D33}^{\varepsilon}}^{(1)} & 0\\ 0 & h_{N,1}\overline{\epsilon_{D33}^{\varepsilon}}^{(N)}\end{bmatrix} \quad \left[\overline{\Psi}\right]=\begin{bmatrix}\overline{\psi}^a z_1 h_{1,1} & 0\\ 0 & \overline{\psi}^s z_N h_{N,1}\end{bmatrix} \tag{34}$$

Table 2. Numerical integration for terms of second equilibrium equation using Gauss-Legendre quadrature

Matrices	Numerical integration
$[\mathbb{Q}_e]$	$\sum_{i=1}^{npt}\sum_{j=1}^{npt}\left[\mathbb{B}^{\varphi}\left(\vec{x}(\xi_i,\eta_j)\right)\right]^T[\mathbb{Z}]\left[\mathbb{B}^{\varphi}\left(\vec{x}(\xi_i,\eta_j)\right)\right]J(\xi_i,\eta_j)W_iW_j$
$\vec{F}_e^E$	$\sum_{i=1}^{npt}\left[\overline{\Psi}\right]\left[\mathbb{B}^{\varphi}\right]J\left(\tau_i\right)W_i$

Using Galerkin finite element method, it is possible to obtain the discrete equations presented in Eq. 35 and Eq. 36.

$$\left\{\sum_e[\mathbb{M}_e]\left\{\overrightarrow{\ddot{q}}_e\right\}+\sum_e\left[[\mathbb{K}_e]+[\mathbb{H}_e^{qu}]\right]\{\vec{q}_e\}\right\}\{\delta\vec{q}_e\}=\sum_e\left\{\vec{F}_e^{gu}-\vec{F}_e^{g\theta}+\vec{F}_e^N-\vec{F}_e^M\right\}\{\delta\vec{q}_e\} \tag{35}$$

$$\text{and}\quad\sum_e\left[\mathbb{K}_e^E\right]\{\vec{q}_e\}\{\delta\vec{q}_e\}=\sum_e\left\{\vec{F}_e^E\right\}\{\delta\vec{q}_e\} \tag{36}$$

$$\text{where}\quad[\mathbb{M}_e]=[\mathbb{M}_e^u]+\left[\mathbb{M}_e^{\theta}\right]-\left[\mathbb{M}_e^{u\theta}\right];\quad[\mathbb{K}_e]=\left[\mathbb{K}_e^P\right]+\left[\mathbb{K}_e^S\right];\quad\left[\mathbb{K}_e^E\right]=[\mathbb{Q}_e]+[\mathbb{H}_e^{qu}]^T \tag{37}$$

Assembling all degrees of freedom, results in global matrix presented in Eq. 38.

$$\begin{bmatrix}\mathbb{M}&0&0\\0&0&0\\0&0&0\end{bmatrix}\begin{Bmatrix}\overrightarrow{\ddot{U}}\\\overrightarrow{\ddot{\phi}}_1\\\overrightarrow{\ddot{\phi}}_N\end{Bmatrix}+\begin{bmatrix}\mathbb{K}_U&\mathbb{K}_{U\phi}^{(1)}&\mathbb{K}_{U\phi}^{(N)}\\\mathbb{K}_{\phi U}^{(1)}&\mathbb{K}_{\phi}^{(1)}&0\\\mathbb{K}_{\phi U}^{(N)}&0&\mathbb{K}_{\phi}^{(N)}\end{bmatrix}\begin{Bmatrix}\vec{U}\\\vec{\phi}_1\\\vec{\phi}_N\end{Bmatrix}=\begin{Bmatrix}\vec{F}_{ext}^{mec}\\\vec{F}^1\\\vec{F}^N\end{Bmatrix} \tag{38}$$

Now, it is possible to separate sensor and actuator equations and dynamically analyse their effect in the structure. The sensor works according to direct piezoelectric mode, i.e., mechanical loads induce electric charge generation in its interior. Then, sensor will not produce electrical forces inducing mechanical strains in the structure. This assumption is reliable since the electric potential generated is very weak (normally smaller than $1V$). This assumption leads to the Eq. 39.

$$\left[\mathbb{K}_{\phi U}^{(S)}\right]\left\{\vec{U}\left(t\right)\right\}+\left[\mathbb{K}_{\phi}^{(S)}\right]\left\{\vec{\phi}_S\left(t\right)\right\}=0 \tag{39}$$

Substituting Eq. 39 in Eq. 38, and considering that structure presents proportional damping, leads to Eq. 40.

$$[\mathbb{M}]\left\{\overrightarrow{\ddot{U}\left(t\right)}\right\}+[\mathbb{C}]\left\{\overrightarrow{\dot{U}\left(t\right)}\right\}+\left[[\mathbb{K}_U]-\left[\mathbb{K}_{U\phi}^{(S)}\right]\left[\mathbb{K}_{\phi}^{(S)}\right]^{-1}\left[\mathbb{K}_{\phi U}^{(S)}\right]\right]\left\{\vec{U}\left(t\right)\right\}=\left\{\vec{F}_{ext}^{mec}\left(t\right)\right\}-\left[\mathbb{K}_{U\phi}^{(A)}\right]\left\{\vec{\phi}_A\left(t\right)\right\} \tag{40}$$

where damping matrix is defined as $[\mathbb{C}]=\alpha[\mathbb{M}]+\beta[\mathbb{K}_U]$, with α and β are numerical parameters.

6. VALIDATION

First, mechanical part of the model was validated with isotropic and orthotropic plate. Different combinations of boundary conditions (simply supported and clamped) and loads (concentrated or uniform load) were tested for isotropic and orthotropic plates. Results shown perfect match with those found in (Reddy, 2004), who also used Quad9 elements, and presented a better result than a Quad4 element model exposed in (Kwon and Bang, 1997) comparing to analytical solutions. The developed model is optimum with 8x8 elements mesh for thick plate (width/height = 10) and 4x4 mesh for thin plate (width/height = 100). At last, an orthotropic plate with piezoelectric sensors and actuators was tested. The implementation used commercial software MATLAB® and results were compared with: analytical solutions, results from other works and from commercial software ANSYS®. More details about validation tests can be found in da Silva (2007).

A full explained example is presented in order to validate a structure with sensors and actuators. Here, three actuators were fixed on upper surface and three sensors symmetrically bonded on lower surface. This structure is defined in de Abreu et al. (2004) and represented in Fig. 2. The plate consists of a single isotropic layer and adhesive layers are neglected. The structure dimensions and each material properties are listed in Table 3.

Individual voltage value is applied for each actuator and resulting deformation and sensors potentials are evaluated. Results are compared with a closed form solution proposed by Dimitriadis et al. (1991) and results evaluated by the software ANSYS®(SOLID5 for piezoelectric actuators/sensors and SOLID191 for isotropic plate). Figures 3(a) and 3(b) show the centerline static displacement under $-1V$, $1V$ and $1V$ voltage applied to actuators 1, 2 and 3 respectively along the x-direction and y-direction.

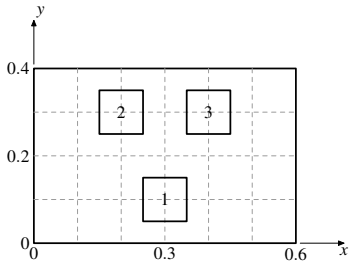

Figure 2. Plate configuration with piezoelectric materials

Table 3. Physical properties of piezoelectric and isotropic materials

Properties	Sensor	Actuator	Plate
Geometry: Lx x Ly (m)	0.1 x 0.1	0.1 x 0.1	0.6 x 0.4
Height: h (mm)	0.205	0.254	1.0
Young's moduli: Y (GPa)	2.0	69.0	207.0
Poisson's ratio: ν	0.3	0.3	0.29
Piezoelectric constants: $e_{31} = e_{32}$ (C/m^2)	-0.046	-12.5	
Dielectric constants (F/m)	1.06 x 10^{-10}	1.60 x 10^{-8}	

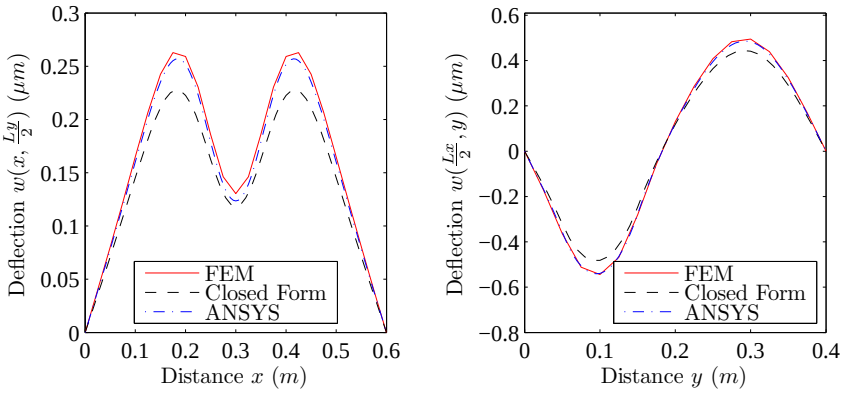

Figure 3. Transversal displacement along x- and y-axis

Table 4. Deflection (μm) and voltage (V) in each sensor.

Sensor	Deflection (μm)			Voltage (V)		
	Closed Form	FEM	ANSYS®	Closed Form	FEM	ANSYS®
1	-0.4816	-0.5440	-0.5392	0.0139	0.0125	0.0126
2	0.6827	0.7747	0.7598	-0.0139	-0.0128	-0.0125
3	0.6827	0.7747	0.7598	-0.0139	-0.0128	-0.0125

A minimal difference is observed between model results and those reported by ANSYS® and a larger difference with those obtained by closed form. This difference derive from the approximation made by analytical solution about the absence of sensor stiffness. Table 4 presents deflection values in sensors centre points and voltage developed in sensors.

The error between developed model and closed form is 13% for displacement and 8% for sensor voltage, which is very close of ANSYS®(12% and 9.5% respectively) error also. A better agreement is found comparing results between implemented and ANSYS®models: 1.5% for displacement and 2% for sensor voltage.

These results prove developed model accuracy and validate static behaviour of the proposed structure.

7. APPLICATION AND CONTROL

This example uses a cantilevered laminate composite plate with upper and lower surfaces symmetrically bonded with piezoelectric ceramics. The goal is to investigate active shape and vibration control effect on composite plate using integrated sensors and actuators. Upper piezoceramic is the sensor and the lower one, the actuator. Structure dimensions and material properties are listed in Table 5.

Table 5. Material properties

Property	Piezoceramic	Composite
Young's modulus along x-direction: Y_1 (GPa)	63.0	150.0
Young's moduli along y- and z-directions: $Y_2 = Y_3$ (GPa)	63.0	9.0
Poisson's ratio: $\nu_{12} = \nu_{13}$	0.3	0.3
Poisson's ratio: ν_{23}	0.3	0.3
Shear moduli: $G_{12} = G_{13}$ (GPa)	24.2	7.10
Shear modulus: G_{23} (GPa)	24.2	2.50
Piezoelectric constants: $(d_{31} = d_{32})$ (m/V)	254 x 10^{-12}	
Dielectric constants: $(\epsilon^{\varepsilon}_{11} = \epsilon^{\varepsilon}_{22})$ (F/m)	15.3 x 10^{-9}	
Dielectric constant: $(\epsilon^{\varepsilon}_{33})$ (F/m)	15.0 x 10^{-9}	

A 8 x 8 element mesh was employed and, in order to perform control, a PID controller was applied. The proportional gain was used to amplify voltage in actuators, provided by closed loop sensors's signal. The integral term was added to cancel the static error induced by the proportional gain. At last, a derivative part was designed to assign a predictive effect in control, aiming to improve system response. The complete structure is presented in Fig. 4. In this condition, the desired sensor voltage is zero. So, resulting voltage in actuator is defined by the Eq. 41.

$$\vec{\phi}_a(t) = -K_p\vec{\phi}_s(t) - K_i\int \vec{\phi}_s(t)\,dt - K_d\frac{d\vec{\phi}_s(t)}{dt} \tag{41}$$

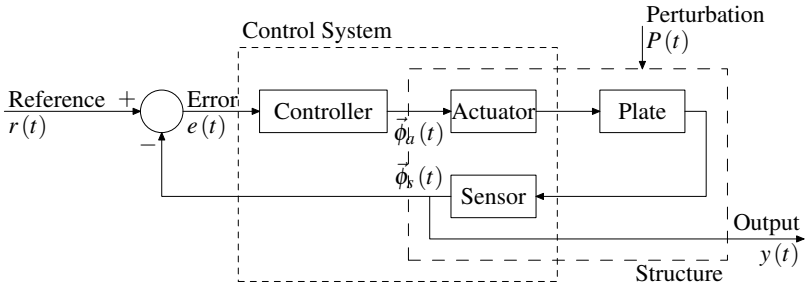

Figure 4. Schematic representation of control system

First, a concentrated force ($\vec{F} = 1N$) is applied as exposed on Fig. 5 and sensor output is analyzed and compared to reference, set as zero. Ziegler and Nichols (1942) tuning method is used to estimate PID gains. In this application, proportional, integrative and derivative gains are 1.6200, 83.9378 and 0.0078, respectively.

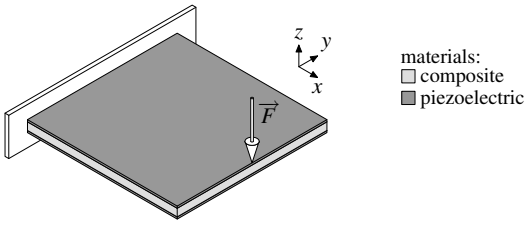

Figure 5. Proposed structure

Figure 6 presents sensor voltage due to continuous force applied in plate edge. In closed loop, amplitude vibration is smaller if compared to open loop response in same instant. Sensor voltage is also tracking reference value in steady state, set as zero, proving that static error in steady state was suppressed. Closed loop response of deflection shows that the structure finds a new position closer to zero at the evaluated point. This confirms that shape control is functional, even if it needs more time to completely perform its effect. This happens because sensor voltage at this stage assumes small values, so the actuator loses efficiency. However, due to PID integrative term, actuator will work until resulting deformation finds its equilibrium point.

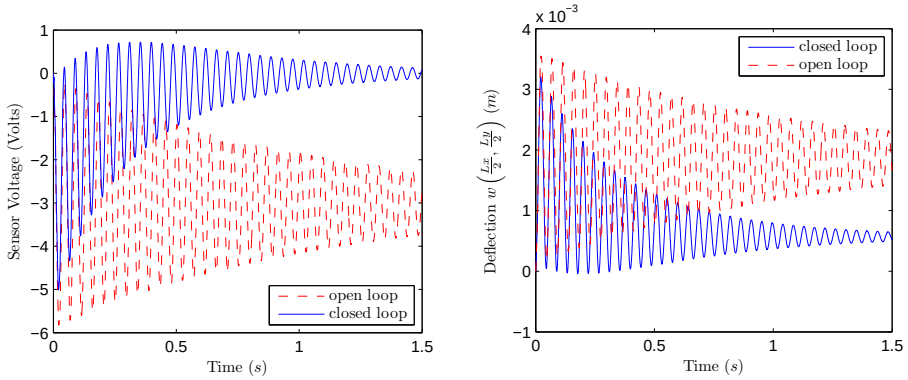

(a) Sensor voltage (b) Deflection

Figure 6. Sensor voltage and deflection in open and closed loop

8. CONCLUSIONS

An efficient finite element model, based on Mindlin's plate theory, is proposed to simulate smart composite structures with piezoelectric materials. Several static and dynamic tests were performed demonstrating the accuracy of the methodology used. The results obtained by this model presents good agreement with analytical solutions and software ANSYS®. The conceived PID controller proved to be able to perform shape and vibration control as required. The presented methodology is an useful tool for designing active vibration control devices.

9. REFERENCES

Adriaens, H. J. M. T. A., de Koning, W. L., & Banning, R., 2000. Modeling piezoelectric actuators. *IEEE/ASME Transactions on Mechatronics*, vol. 5, n. 4, pp. 331–341.

Bathe, K.-J. & Wilson, E. L., 1976. *Numerical Methods in Finite Element Analysis*. Prentice-Hall, Inc., Englewood Cliffs, New Jersey.

Bhattacharya, P., 2006. Effects of piezo actuated damping on parametrically excited laminated composite plates. *Journal of Reinforced Plastics and Composites*, vol. 25, n. 8, pp. 801–813.

da Silva, F. C. G., 2005. Indirect force measurement using a piezoelectric actuator. Monografia, Universidade Federal de Santa Catarina, Florianópolis, Brasil.

da Silva, F. C. G., 2007. Modelagem de uma placa de materiais compósitos e piezelétricos pelo método dos elementos finitos. aplicação de controle de vibração. Master's thesis, Universidade Federal de Santa Catarina.

de Abreu, G. L. C. M., Ribeiro, J. F., & Steffen, Jr, V., 2004. Finite element modeling of a plate with localized piezoelectric sensors and actuators. *Journal of the Brazilian Society of Mechanical Sciences and Engineering*, vol. 26, n. 2, pp. 117–128.

Dimitriadis, E. K., Fuller, C. R., & Rogers, C. A., 1991. Piezoelectric actuators for distributed vibration excitation of thin plates. *Transactions of the ASME*, vol. 113, pp. 100–107.

Kwon, Y. W. & Bang, H., 1997. *The Finite Element Method Using Matlab*. CRC Press, 1 edition.

Lam, K. Y., Peng, X. Q., Liu, G.-R., & Reddy, J. N., 1997. A finite element model for piezoelectric composite laminates. *Smart Materials and Structures*, vol. 6, n. 5, pp. 583–591.

Reddy, J. N., 1999. On laminated composite plates with integrated sensors and actuators. *Engineering Structures*, vol. 21, n. 7, pp. 568–593.

Reddy, J. N., 2004. *An Introduction to Nonlinear Finite Element Analysis*. Oxford University Press, 1 edition.

Ziegler, J. G. & Nichols, N. B., 1942. Optimun settings for automatica controllers. *Transactions of the ASME*, vol. 64, pp. 759–768.

10. Responsibility notice

The author(s) is (are) the only responsible for the printed material included in this paper.